

Pax transactivation domain-interacting protein is required for preserving hematopoietic stem cell quiescence via regulating lysosomal activity

Tong Zhang,^{1,2*} Manman Cui,^{1,2*} Yashu Li,^{1,2} Ying Cheng,^{1,2} Zhuying Gao,¹ Jing Wang,¹ Tiantian Zhang,^{1,2} Guoqiang Han,^{1,2} Rong Yin,³ Peipei Wang,^{1,2} Wen Tian,^{1,2} Weidong Liu,¹ Jin Hu,^{1,2} Yuhua Wang,¹ Zheming Liu⁴ and Haojian Zhang^{1,2,5}

¹The State Key Laboratory Breeding Base of Basic Science of Stomatology and Key Laboratory of Oral Biomedicine Ministry of Education, School and Hospital of Stomatology, Medical Research Institute, Wuhan University; ²Frontier Science Center for Immunology and Metabolism, Wuhan University; ³Department of Hematology, Zhongnan Hospital, Wuhan University; ⁴Cancer Center, Renmin Hospital, Wuhan University and ⁵Taikang Center for Life and Medical Sciences, Wuhan University, Wuhan, China

*TZ and MC contributed equally as first authors.

Correspondence: H. Zhang
haojian_zhang@whu.edu.cn

Z. Liu
ZhemingLiu@whu.edu.cn

Received: October 4, 2022.

Accepted: March 3, 2023.

Early view: March 16, 2023.

<https://doi.org/10.3324/haematol.2022.282224>

©2023 Ferrata Storti Foundation

Published under a CC BY-NC license



Supplementary Data

Supplementary methods

FACS Analysis and Sorting

Total BM cells were isolated from mice's femur and tibia. In brief, two million BM cells were lysed with RBC to remove red blood cells. For HSC, cells were stained with biotin-conjugated lineage markers, then stained with APC-eFlour780-anti-streptavidin, PE-anti-c-Kit, APC-anti-Sca-1, PE-Cy5-anti-CD135, PE-Cy7-anti-CD48, FITC-CD150, PE-CF594-anti-CD41. For CLP, LSKs were additionally stained with CD135 and FITC-anti-CD127. For LK subpopulations, LSKs were additionally stained with FITC-anti-CD34 and PE-Cy7-anti-CD16/32. For mature cells, BM and PB cells were stained with APC-anti-CD4, FITC-anti-CD8, PE-anti-CD11b, APC-Cy7-Gr-1, and PE-Cy5-anti-B220. BD sorters FACS Aria III; BD analyzers FACSCelesta, FACSLSRFortessaX20, and Beckman CytoFlex were used.

***In vivo* treatment assays**

Tgfb1 inhibitor LY364947 (S2805; Selleckchem) was intraperitoneally injected at 2mg/kg. Lysosome protease inhibitor Leupeptin (L2884; Sigma) was intraperitoneally injected at 40mg/kg.

TGFβ1 in vitro treatment assays

Lin^c-kit⁺ cells isolated from WT and Ptip mice were cultured in StemSpan (StemCell Technologies) supplemented with mTPO and mSCF and treated with or without TGFβ1 5 days, and the cells were used calculated for total cell numbers, or harvested for FACS or WB.

Genotyping and Quantitative RT-PCR (RT-qPCR)

For genotyping, Mice's tails were lysed in lysis buffer with Proteinase K, then genotyped by PCR.

For Ptip genotyping primers were Forward: AGACAGCAGTCCCGAATCTGAGC; Reverse:

CAGCAGTAGAAGGTTTCCAAACAT. Scl-CreER genotyping primers were Forward:

GAGTGATGAGGTTTCGCAAGA; Reverse: CTACACCAGAGACGGAAATC. For RT-qPCR

analysis, Total RNA from HSC/HSPCs was purified using TRIzol (Life Technologies) according

to the manufacturer's instructions. Total RNA was reversely transcribed using the ReverTra Ace

qPCR RT Kit (TOYOBO). The levels of specific RNAs were measured using Bio-Rad real-time

PCR machine and Fast SYBRGreen PCR mastermix according to the manufacturer's

instructions. Primer sequences are listed in Supplementary Information Table S1. The 2^{-ΔΔCt}

method was used to normalize expression to Gapdh and actin for cells.

RNA sequencing (RNA-seq) and data analysis

For RNA-seq, LT-HSCs were sorted from WT and Ptip^{-/-} mice bone marrow. Total RNA was

harvested using Trizol reagent. RNA was reverse transcribed with oligo dT primers and

template-switching oligos, followed by amplification by PCR of 12-15 cycles with ISPCR oligos.

The PCR program was as follows: 98°C for 3 min; 10-14 cycles of 98°C 20 s, 67°C 15 s, and

72°C 6 min; 72°C 5 min and 4°C cold. The amplified cDNAs were purified using AMPure XP beads to abolish primer dimers. After purification, 50 ng cDNAs were fragmented using the TruePrep DNA Library Prep Kit. Then the fragments were amplified with N5 primers and N7 primers. The PCR program was as follows: 72°C 3min, 98°C 30 s; 5-9 cycles of 98°C 15 s, 60°C 30 s, and 72°C 3 min; 72°C 5 min and 4°C Cold. After PCR, samples were purified using 1.0 volumes of AMPure XP beads, the cDNA libraries were ready for sequencing on an Illumina HiSeq X Ten sequencing platform. For RNA-seq analysis, reads were mapped to mouse genome version 38 (GRCm38) with Hisat2 (v2.1.0) , and FeatureCounts (v1.6.4) was used to calculate counts from bam files. DESeq2(v1.26.0) was employed for data normalization and differential expression analysis of RNA-seq counts.

Statistical analyses

All the experiments were analyzed using a two-way Student's t-test. For the comparison of different specimens, the unpaired t-test was used. For the comparison of different treatments within the same specimen, the paired t-test was used. The log-rank test was used to compare survival curves. P values of less than 0.05 were considered statistically significant. In the figures, asterisks indicate * $p < 0.05$, ** $p < 0.01$, and *** $p < 0.001$; ns means no significance.

Supplementary Figure legends

Figure S1. Conditional knockout Ptip in Mx1-Cre induced model leads to strong extramedullary hematopoiesis.

(A) Single-cell RNA-seq data showing PTIP expression in healthy donor-derived bone marrow cells. Each dot represents one cell (GSE116256).

(B) Scheme for generating Mx1-Cre; *Ptip* conditional knockout mice.

(C) Gross morphology of spleens and tibias.

(D) qRT-PCR analysis showing the efficiency of *Ptip* deletion in LT-HSC cells at 4 weeks after pIpC treatment.

(E) Representative fluorescence-activated cell sorting plots showing the gating strategy for different stem and progenitor cell population in BM from WT and *Ptip*^{-/-} mice at 4 weeks after pIpC treatment.

(F) Percentages and total numbers of different stem cell populations in bone marrow at 4 weeks after pIpC treatment from WT and *Ptip*^{-/-} mice (n = 4).

Figure S2. Specific knockout *Ptip* in LT-HSC does not arouse extramedullary hemopoiesis and leads to HSC expansion

(A) Scheme for generating Scl-CreER⁺; *Ptip*^{flox/flox} conditional knockout mice.

(B) qRT-PCR analysis showing the efficiency of *Ptip* deletion in LT-HSC cells at 4 weeks after Tamoxifen treatment.

(C) Total cell number counting of BM and SP (left panel: BM (n=10); right panel: SP (n=5)), and blood count analysis in the PB of WT and *Ptip*^{-/-} mice at 4 weeks after tamoxifen treatment (n = 13-14).

(D) Percentages of different populations of mature lineage cells in PB, BM, and SP of WT and *Ptip*^{-/-} mice at 4 weeks after tamoxifen treatment (PB and BM, n = 10; SP, n = 4-5).

(E) Frequencies of different stem and progenitor cell populations in BM from WT and *Ptip*^{-/-} mice at 4 weeks after tamoxifen treatment (n=10).

(F) Total cell numbers (low) of different stem and progenitor cell populations in BM from WT and *Ptip*^{-/-} mice at 4 weeks after tamoxifen treatment (n=10).

Figure S3. Loss of *Ptip* reduces HSC long-term competitive activity in vivo.

(A) Representative peripheral blood analysis of the chimeric mice was performed by flow cytometry after the bone marrow transplantation from WT and *Ptip*^{-/-} mice at 16 weeks.

(B and C) Percentage and total numbers of donor-derived stem cell (left) and progenitor (right) compartments in the bone marrow of recipients at 16 weeks after BMT.

(D) Homing assay showing the comparable homing capability of WT and *Ptip*^{-/-} BM. Flow cytometry analysis for different donor-derived cells in BM of recipient mice at 24h after BMT (n = 5).

Figure S4. Loss of *Ptip* leads to an increase lysosomal degradative potential

(A) Volcano map showing differential expression of *Ptip* targets in WT and *Ptip*^{-/-} LT-HSCs.

(B) Gene ontology (GO) enrichment analysis of terms enriched in different pathways with a significantly up- and down-regulated gene in *Ptip*^{-/-} LT-HSCs.

(C) Gene sets enrichment analysis (GSEA) plot showing enrichment of gene sets of TGF β signaling pathway, Hematopoietic cell lineage, and Cell cycle.

(D) qRT-PCR validation of the effect of Ptip on the expression levels of TGF β targets: *Mycn*, *Myc*, *Cdk6*, *p21*, *p27*, and *p57*.

(E) Representative immunofluorescent confocal images of LAMP2 and DAPI (left; bar, 2 μ m; arrow shows co-localization) and quantification (right; n = 3; 153-193 individual cells).

Figure S5. Ptip coordinates TGF β signaling in regulating HSC quiescence

(A) Pearson's correlation between PTIP and SMAD3 and CDK6 from single-cell RNA-seq data (GSE157591).

(B) Co-immunoprecipitation (CoIP) of HA-SMAD3 and Flag-PTIP from HEK-293 extract the following incubation with HA or Flag antibodies. Immunoprecipitated immunoblotted with the indicated antibodies.

(C) Immunoblotting showing p-Smad2, Smad2/3 expression in total BM cells upon TGF β 1(left) or LY354947(right) treatment.

(D) Co-immunoprecipitation (CoIP) of HA-SMAD3 and Flag-PTIP from HEK-293 extract the following incubation with HA or Flag antibodies. Cells were treated with TGF β 1 and LY364947 respectively. Immunoprecipitated immunoblotted with the indicated antibodies.

(E) Comparison of LT-HSC cell cycle stage (n =4) after TGF β signaling inhibition with LY364947.

(F) qRT-PCR validation of the effect of *Ptip* on the expression levels of Lysosome targets: *Cdk6*, *c/n-Myc*, *p21*, *p27* and *p57* upon PBS and TGFβ1 treatment.

(G) qRT-PCR validation of the effect of *Ptip* on the expression levels of Lysosome targets: *Dram2*, *Ctsd*, *Gm2a* and *Ctsb* upon PBS and TGFβ1 treatment.

Supplementary Table S1 Primer sequences using in this study

Name	Sequence 5'-3'
<i>Ptip-F</i>	CCGAAGTTCAGAGGAGCTA
<i>Ptip-R</i>	AATAACCTGCGGGTCGATGT
<i>Cdk6-F</i>	CTGGTGTGAGATGTTATCATT
<i>Cdk6-R</i>	TAGTCAGAGCAGGAAGTG
<i>P21-F</i>	AATCCTGGTGTGATGCCGACC
<i>P21-R</i>	TTGCAGAAGACCAATCTGCG
<i>P27-F</i>	TATGGAAGAAGCGAGTCAGC
<i>P27-R</i>	GCGAAGAAGAATCTTCTGCAG
<i>P57-F</i>	AGGTAGCGAGGTGGATCTGTC
<i>P57-R</i>	GGCCTCTGATTCGAGGA
<i>Tfeb-F</i>	CCACCCAGCCATCAACAC
<i>Tfeb-R</i>	CAGACAGATACTCCCGAACCTT
<i>Myc-F</i>	ATGCCCTCAACGTGAACCTC
<i>Myc-R</i>	CGCAACATAGGATGGAGAGCA
<i>Dram2-F</i>	GCTGTCCTTGCTTTAGTATGG
<i>Dram2-R</i>	AGATAACCAACAGTAGTCGGACC
<i>Ankrd27-F</i>	TGGCATTGTCCTAGTGCCTTG
<i>Ankrd27-R</i>	AGCCTTCCATCTAAGGTCTGA
<i>Smpd1-F</i>	TGGGACTCCTTTGGATGGG
<i>Smpd1-R</i>	CGGCGCTATGGCACTGAAT
<i>Gns-F</i>	CGGTGTGCGGCTATCAGAC
<i>Gns-R</i>	CAGGGCATAACCAGTAACTCCA
<i>Ctsb-F</i>	GAAGTCCCAGCTTGAATCGAAAGAA
<i>Ctsb-R</i>	TAGGAAGACAGGGTCAAAGGCTTGT
<i>Mycn-F</i>	ACCATGCCGGGGATGATCT
<i>Mycn-R</i>	AGCATCTCCGTAGCCCAATTC
<i>Gapdh-F</i>	TGGATTTGGACGCATTGGTC
<i>Gapdh -R</i>	TTTGCACTGGTACGTGTTGAT

Figure S2

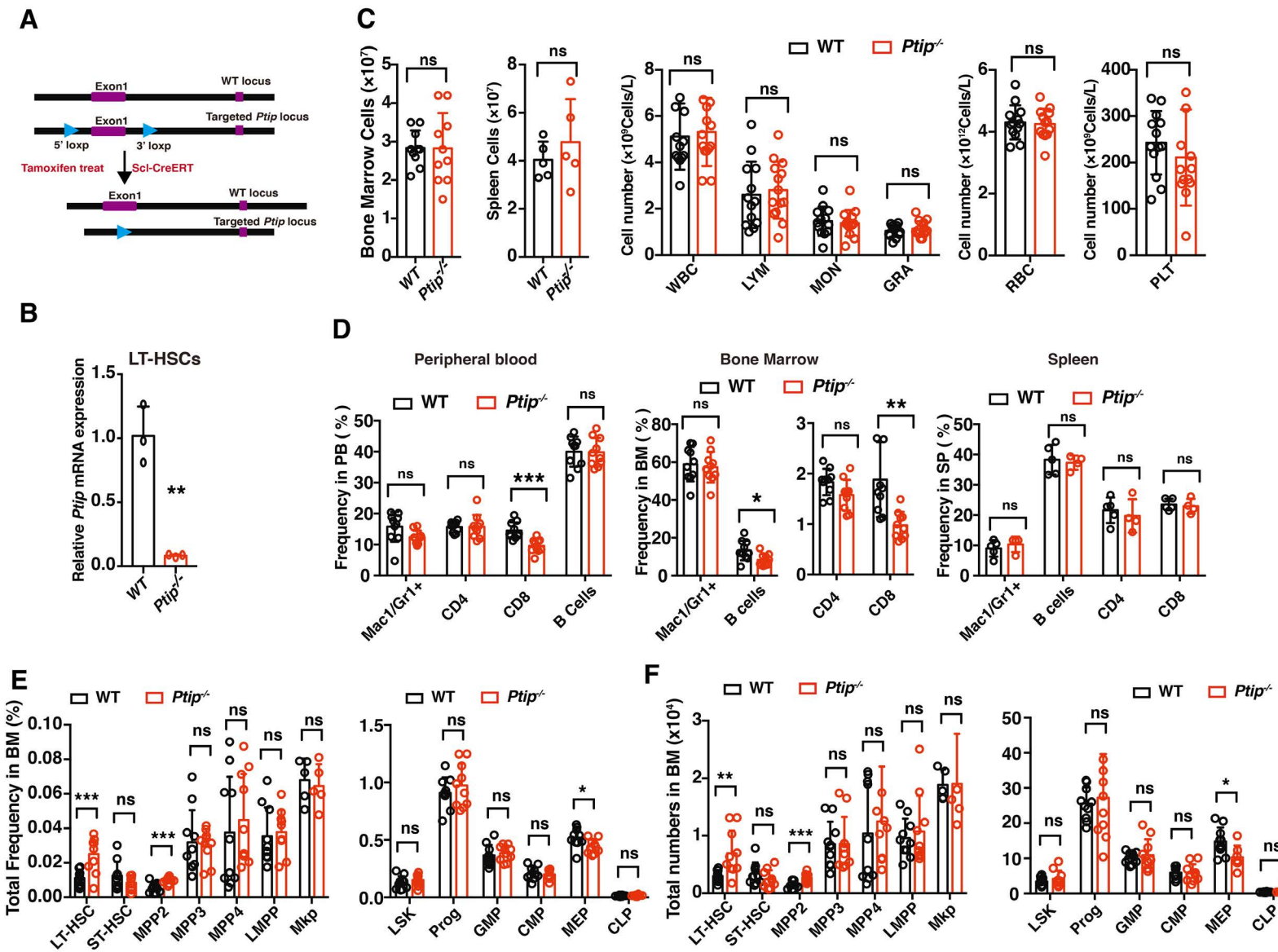
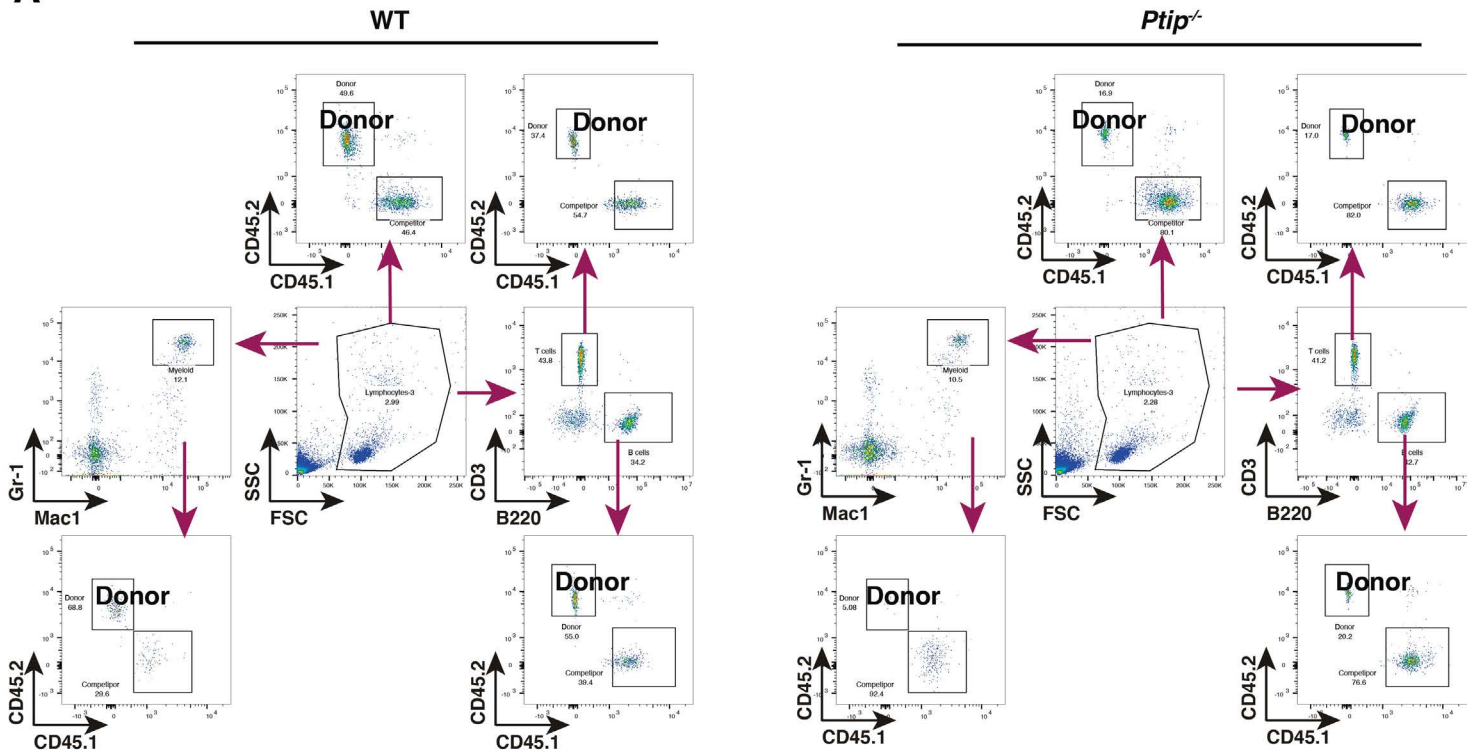
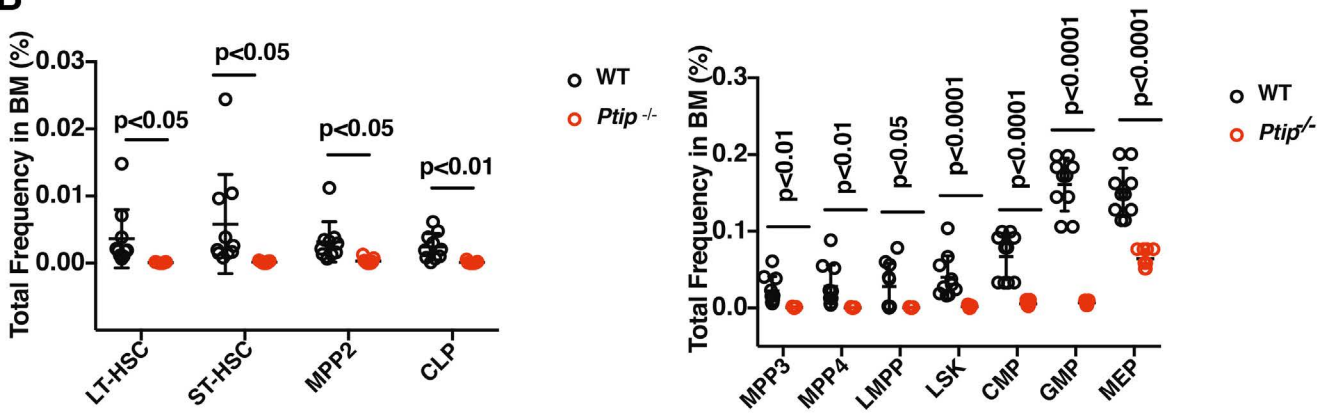


Figure S3

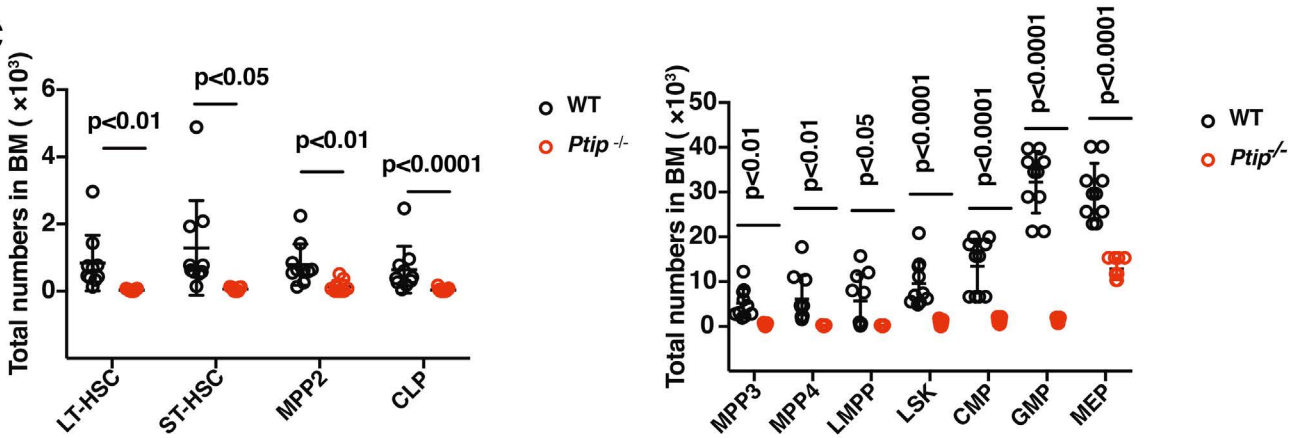
A



B



C



D

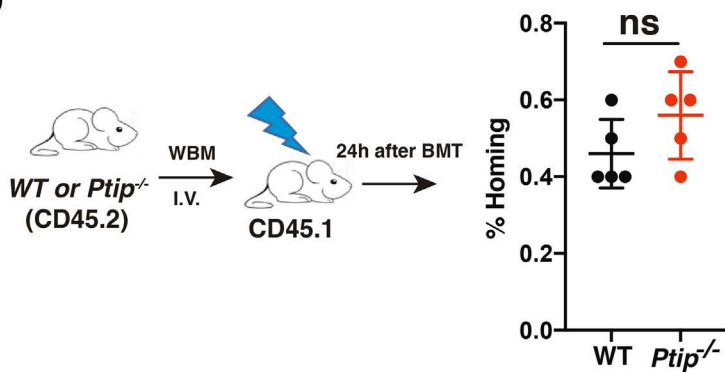


Figure S4

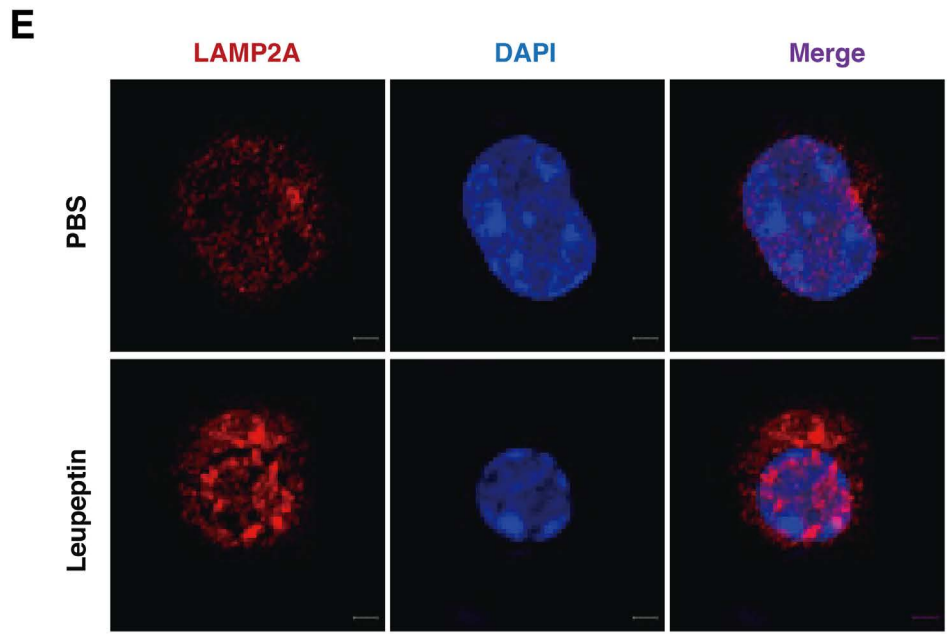
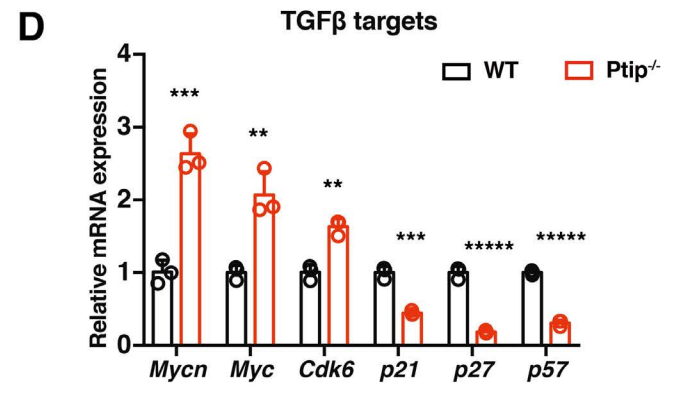
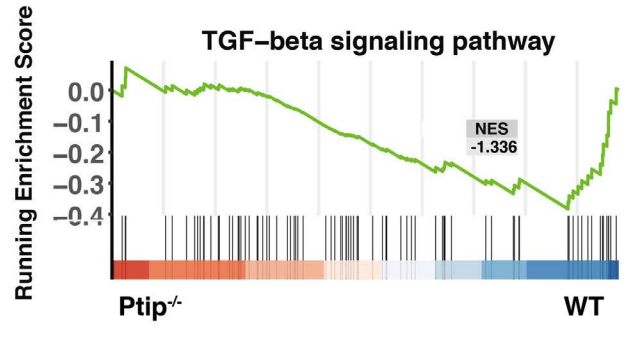
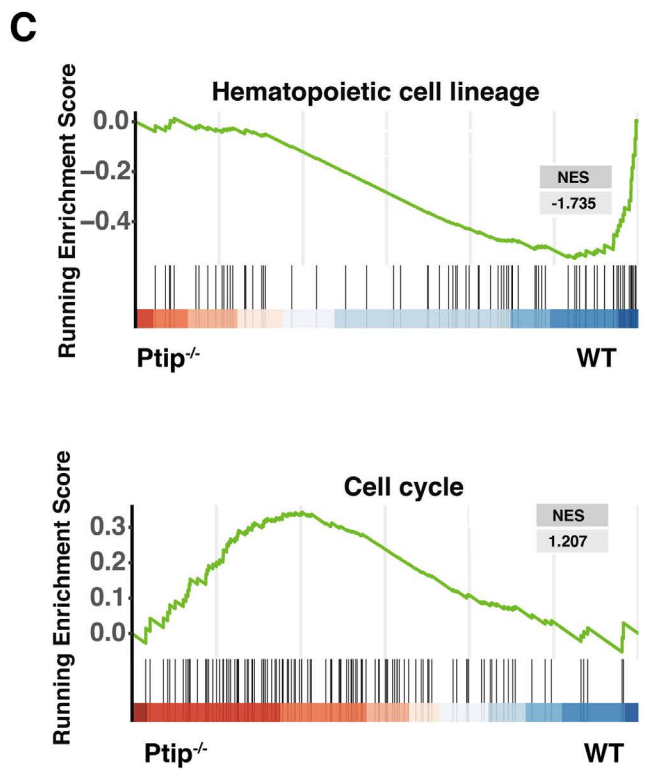
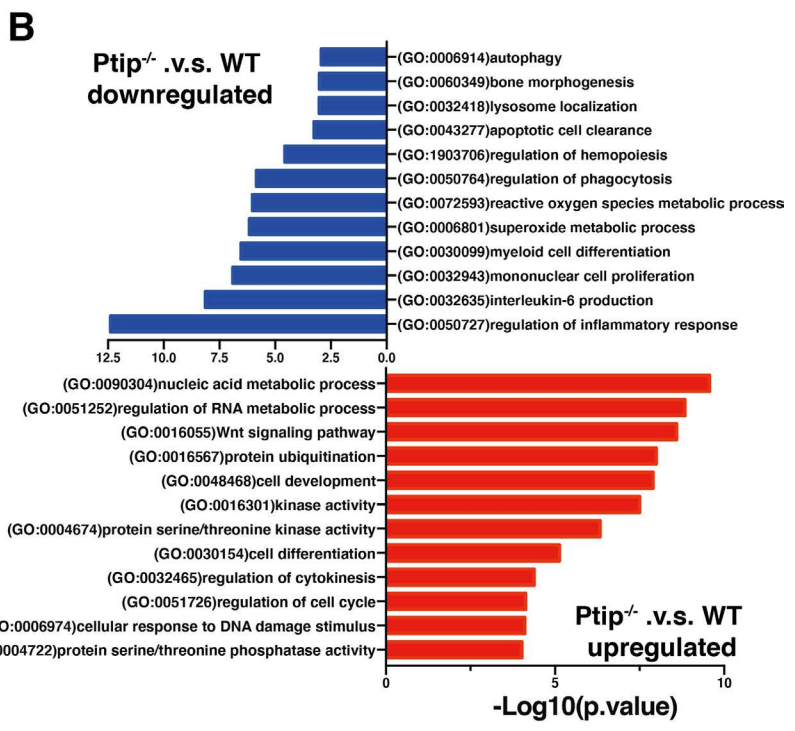
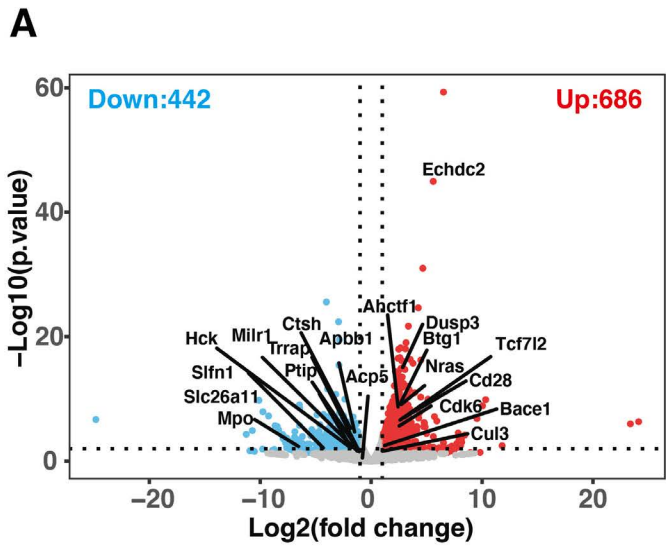
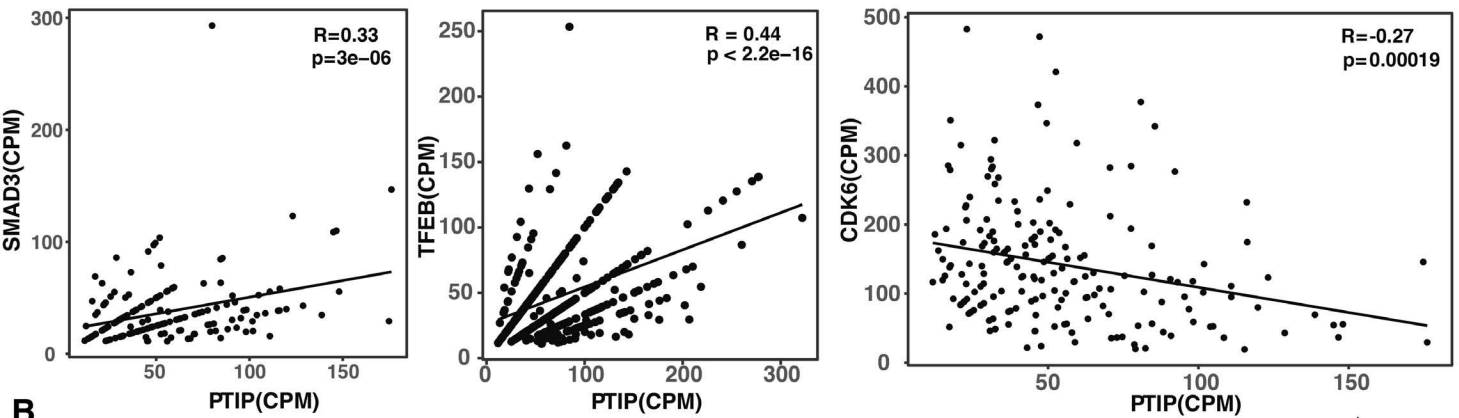
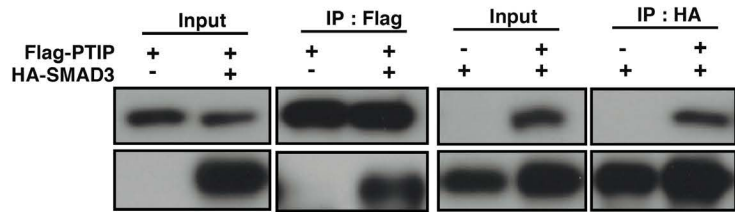


Figure S5

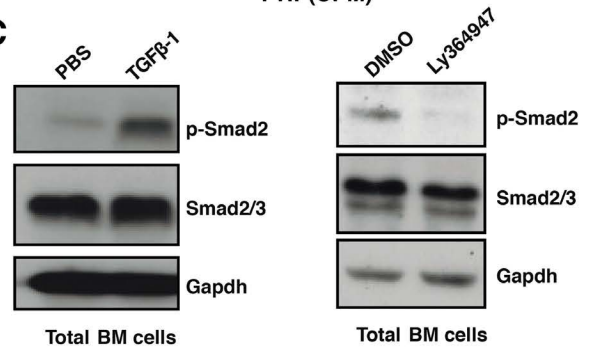
A



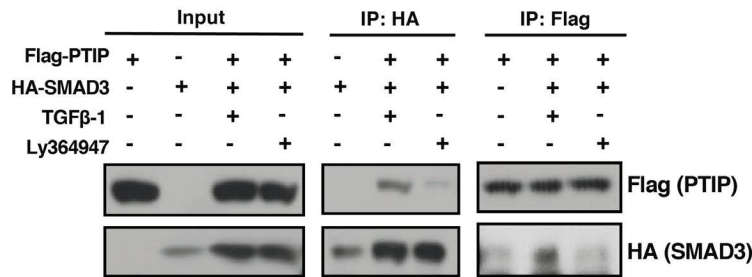
B



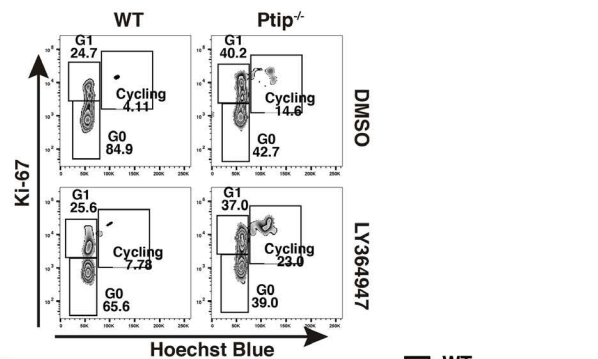
C



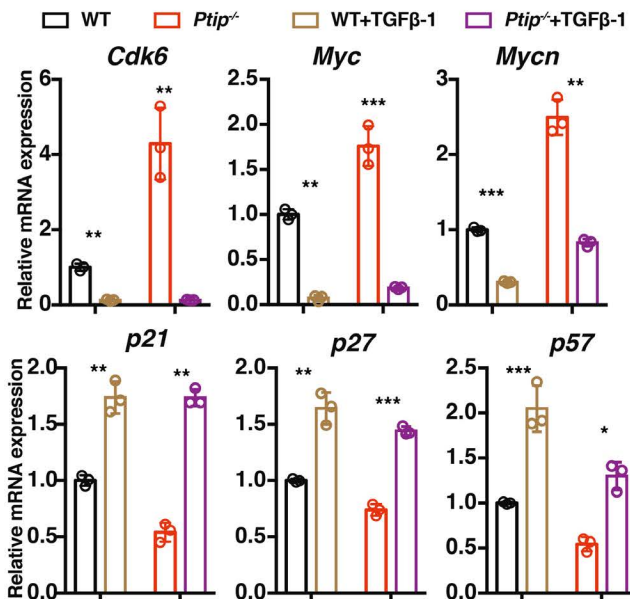
D



E



F



G

